

Article

An Investigation on the Usability of Acceleration Test by Impressed Anodic Current for Evaluating Corrosion Behavior of Hot-Dip Galvanized Rebar in Concrete

Hong-bok Choe ^{1,*}, Yuhei Nishio ² and Manabu Kanematsu ^{2,*}

¹ Department of Architecture, Graduate School of Science and Technology, Tokyo University of Science, 2641 Yamazaki, Noda, Chiba 278-8510, Japan

² Department of Architecture, Faculty of Science and Technology, Tokyo University of Science, 2641 Yamazaki, Noda, Chiba 278-8510, Japan; y.nishio@rs.tus.ac.jp

* Correspondence: hongbokchoe@gmail.com (H.-b.C.); manabu@rs.noda.tus.ac.jp (M.K.); Tel.: +81-4-7124-1501 (ext. 3507) (M.K.)

Received: 27 September 2019; Accepted: 28 October 2019; Published: 30 October 2019



Abstract: Hot-dip Galvanized rebar (hereafter, HDG rebar) has an anti-corrosion effect due to the sacrificial anodic reaction of zinc. Additionally, the zinc coating itself provides barrier protection for the steel substrate. Meanwhile, from one of the investigations on the field performance of HDG rebar in concrete, HDG rebar did not protect the substrate when the remaining zinc was under 50 μm . For the evaluation of this property over a short period of time, an acceleration test using impressed anodic current (hereafter, acceleration test) may be useful. This test impresses constant direct current into the rebar and can result in the intended quantitative extent of the anodic reaction. However, in using this test on HDG rebar, it was found that the high rate of applied current density could cause an unintended early end of the anti-corrosion effect of zinc, despite there being more than 50 μm of remaining zinc thickness. In this study, the usability of the acceleration test was investigated to determine if it is a suitable method for evaluating the anti-corrosion behavior of HDG rebar in concrete. As a test variable, a comparatively low rate of applied current density was used in the experiments. As a result, it was clarified that an effective corrosion protection of the substrate was made with an increase of the zinc corrosion amount. This anti-corrosion effect was similar to that known to exist in actual corrosion environments. This behavior was terminated when the concrete cracked, and the substrate became corroded. While the test condition in this study resulted in an early end of the anti-corrosion effect of zinc, a linear correlation was achieved between the applied current density and the remaining zinc thickness at the time that the anti-corrosion effect was terminated. It was found that lowering the applied current density resulted in a more suitable test condition. In conclusion, the acceleration test was found to be useful, although further experimental validation is necessary to confirm this finding.

Keywords: hot-dip galvanized rebar; impressed anodic current; applied current density; polarization resistance; zinc coating thickness

1. Introduction

Currently, studies on the anti-corrosion performance of hot-dip galvanized rebar (hereafter, HDG rebar) in concrete have been carried out [1–8]. HDG rebar is a zinc-coated steel reinforcement. It is known to have an anti-corrosion effect due to the sacrificial anodic reaction of zinc. Since zinc is electrochemically a more active metal than iron, zinc corrodes itself, replacing the steel substrate and

suppressing the corrosion of steel. This reaction also works on a damaged surface (exposed substrate). Furthermore, the zinc coating itself provides barrier protection for the steel substrate. For this reason, HDG rebar has been expected to have a long-term corrosion protection service life [1–4].

Concerning this anti-corrosion behavior, investigations on the field performance of HDG rebar in aged concrete have been carried out as well. On the aged concrete, which was from 3–28 years old, most of them indicated that the HDG rebar showed a sufficient amount of remaining zinc thickness, with negligible or a little corrosion of the substrate [9–13]. Meanwhile, from one of the investigations, which was the result at Tioga bridge in Pennsylvania (17-year-old concrete), a sample showed severe surface cracking, and the zinc thickness was 38 μm [12]. Additionally, though it was the result of a cyclic salt water wetting and drying test for 20–60 months (0.7 water/cement ratio concrete cylinder, 45–100 μm of zinc coating thickness), the HDG rebar, which was below a zinc thickness of 50 μm , showed corrosion of the substrate [14]. From this result, it was shown that the HDG rebar did not protect the substrate, when the remaining zinc was below 50 μm .

For the evaluation of this property over a short period of time, an acceleration test using impressed anodic current (hereafter, acceleration test) may be useful. This test uses a direct current (hereafter, DC) power supply to impress constant direct current into the rebar and results in an intended anodic reaction in a quantitative way. Besides, it can adjust the total current amount ($\text{mA} \times \text{h}/\text{cm}^2$) and applied current density (mA/cm^2). Because of this characteristic, the acceleration test has been used to evaluate the corrosion behavior or the structural performance of ordinary rebar [15–20] and HDG rebar as well, along with the embedded state in concrete [21–26].

However, in using this test on HDG rebar, Niwa et al. [6] found that the high rate of the applied current density could cause an unintended early end of the anti-corrosion effect of zinc. In their study, 0.625 mA/cm^2 of the current density was impressed to corrode the HDG rebar, of which the coating thickness was 153 μm . As a result, after 43% of the actual corrosion amount occurred, the substrate started to corrode, and the anti-corrosion effect did not function. At this stage, the remaining zinc thickness was 87 μm . From this result, it was found that the anti-corrosion performance of HDG rebar could be underestimated by the influence of the applied current density.

In this study, the usability of the acceleration test was investigated, considering if it is a suitable method for evaluating the anti-corrosion behavior of HDG rebar in concrete. As a test variable, the comparatively low rate of applied current density was used in the experiments. Additionally, the water/cement ratio of concrete (hereafter, w/c) and the total current amount were considered as variables. After the acceleration test, the polarization resistance and corroded amount of zinc were evaluated for comparison with previous studies.

2. Materials and Methods

2.1. Experimental Scope

Table 1 shows the specimen list and experimental variables. In this study, the w/c , applied current density, and designed corrosion amount (hereafter, DCA) were considered as variables.

Concerning w/c , concretes were prepared with $w/c = 50\%$ and $w/c = 83.5\%$, which allows for the investigation of whether the concrete mix proportion influences the corrosion extent of HDG rebar. When $w/c = 83.5\%$, concrete is the same condition as that was used in the study of Niwa et al. [6].

Concerning the applied current density, 0.16, 0.08 and 0.02 mA/cm^2 were impressed on $w/c = 50\%$ concrete. On $w/c = 83.5\%$ concrete, 0.08 and 0.23 mA/cm^2 were impressed. 0.08 mA/cm^2 was considered the same acceleration condition as that between $w/c = 50\%$ and 83.5% concrete. In this experiment, the current impressed by a DC power supply was 10 mA on all specimens to provide the lowest anodic current possible. Therefore, the applied current density (mA/cm^2) was adjusted by the surface area (cm^2) of the HDG rebar of each specimen.

Concerning DCA, 10%–100% of DCA was considered. On each specimen, 25%, 50%, 75%, and 100% were the most important test conditions. DCA indicates an estimated corrosion thickness of zinc

coating, which is estimated by the total current amount ($\text{mA} \times \text{h}/\text{cm}^2$) of the acceleration test. A DCA of 100% indicates a full consumption of the zinc coating formed on HDG rebar. The measurement result using the thickness meter showed that $180 \mu\text{m}$ of the zinc coating was formed when it was in a non-corroded state. Therefore, 100% of DCA indicated a zinc corrosion of $180 \mu\text{m}$, which was considered as the reference thickness. In this study, the DCA focused on the anodic reaction of zinc only, which is the stage before the corrosion of the substrate.

Table 1. Specimen list and experimental variables.

No	Specimen	W/C (%)	Applied Current Density (mA/cm^2)	Surface Area of HDG Rebar (cm^2)	DCA ² (%)
1	1-1	50	0.16	62.5	25
	1-2				50
	1-3				75
	1-4				100
2	2-1	50	0.08	125	25
	2-2				50
	2-3				75
	2-4				100
3	3-1	50	0.02	500	25
	3-2				50
	3-3				75
4	4-1	50	0.08	125	15
	4-2				25
	4-3				50
	4-4				100
5	5-1	83.5	0.23	43.5	10
	5-2				25
	5-3				50
	5-4				85
	5-5				100
6	6-1	83.5	0.23	43.5	25
	6-2				50
	6-3				85

¹ W83.5-D230-1 and W83.5-D230-2 are identical specimens; ² DCA: Designed corrosion amount.

Equations (1) and (2) and Table 2 indicate the process of the estimation of the required total current amount for DCA in this experiment. Equation (1) is Faraday's law [27], which explained the relationship between the corrosion current density and corrosion rate of zinc. Equation (2) was derived based on this relationship, and the (year) was converted into the (hour). Therefore, if the thickness of the zinc coating is known, the acceleration test can show the corrosion extent of HDG rebar quantitatively, as shown in Table 2. From the total current amount ($\text{mA} \times \text{h}/\text{cm}^2$), the acceleration test period (h) was adjusted by the applied current density of each specimen.

$$1 \mu\text{A}/\text{cm}^2 \approx 14.98 \mu\text{m}/\text{year} \quad (1)$$

(Left: corrosion current density; Right: corrosion rate of zinc, calculated by Faraday's law).

$$1 \text{ mA} \times \text{h/cm}^2 \approx 1.71 \text{ } \mu\text{m} \quad (2)$$

(Left: total current amount from the acceleration test; Right: corrosion thickness of the zinc coating).

Table 2. The relationship among DCA, zinc coating thickness and the total current amount.

DCA (%)	Predicted Corrosion Thickness of Zinc Coating (μm)	Required Total Current Amount ($\text{mA} \times \text{h/cm}^2$)
10	18	10.53
15	27	15.79
25	45	26.32
50	90	52.63
75	135	78.95
85	153	89.47
100	180	105.26

2.2. Specimen Preparation and the Acceleration Test

Figure 1 shows the specimen setup. Single deformed rebar was used in this experiment, and the nominal diameter was 15.9 mm (D16). On the concrete, $100 \times 100 \text{ mm}^2$ of the cross-section was made, and the length was prepared, considering the surface area of HDG rebar. On the cross-section of HDG rebar, an electric wire was connected to make the HDG rebar the anode in the acceleration test. After that, both sides were insulated by epoxy adhesive. Table 3 indicates the mix proportion of the concrete used for the specimen.

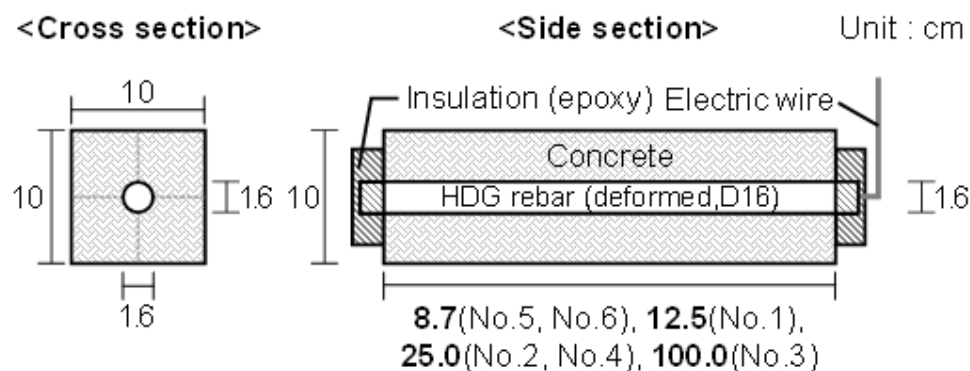


Figure 1. Specimen outline.

Table 3. Mix proportion of concrete for the specimen.

W/C (%)	Unit Weight (kg/cm^3)					Air (%)	Slump Height (cm)	Slump Flow (cm)	Compressive Strength ⁴ (N/mm^2)
	W	C	S ¹	G ²	Ad ³				
50.0	185	370	796	943	1.85	3.0	18.9	32	32.4
83.5	193	232	947	857	2.32	4.1	19.5	34	21.8

¹ Fine aggregate; ² Coarse aggregate; ³ Admixture; ⁴ Compressive strength at 28 days.

Figure 2 shows the composition of the acceleration test. Firstly, a Cu plate was used as a cathode and placed on the bottom of the cell. Secondly, the specimen was immersed in tap water at a certain distance from the plate. Thirdly, the specimen was connected to the (+) terminal, and the Cu plate was connected to the (-) terminal of the DC power supply. Finally, by turning on the device to impress the constant current (10 mA), the test was initiated. While the test was in progress, tap water was periodically supplied to the cell to maintain the wet condition of the specimen.

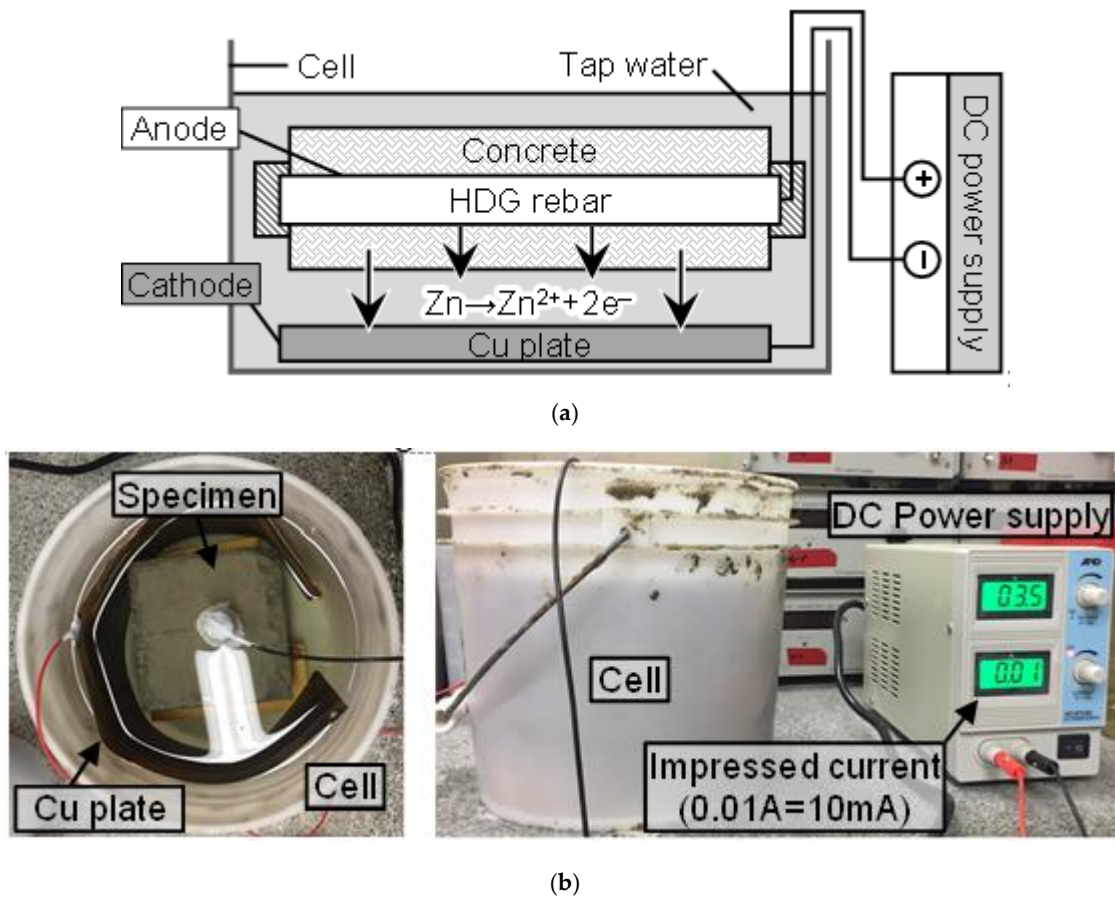


Figure 2. (a) Acceleration test; (b) View of the acceleration test as the current was impressed on the specimen.

In Table 3, the air content (%) was measured by a concrete air meter, and the slump height (cm) and slump flow (cm) was measured by a slump cone. Figure 3 indicates the devices used in the measurement of fresh concrete for the specimens.

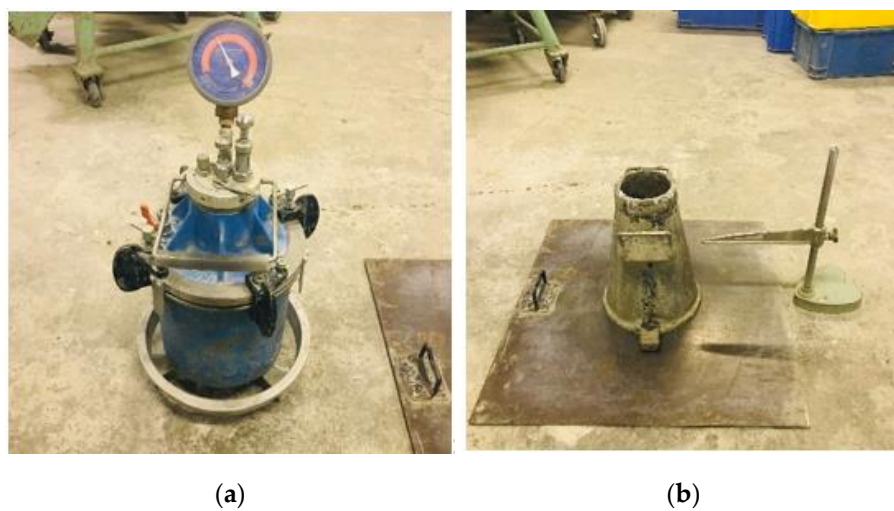


Figure 3. Devices used in the measurement of fresh concrete for the specimens. (a) Concrete air meter; (b) Slump test.

2.3. Polarization Test

Figure 4 shows an outline of the polarization test, which was carried out after the acceleration test to evaluate the electrochemical behavior of HDG rebar. Employing the potentiostatic technique, three electrodes were used, which were the Ag/AgCl electrode (reference), HDG rebar in the specimen (working), and Cu plate (counter).

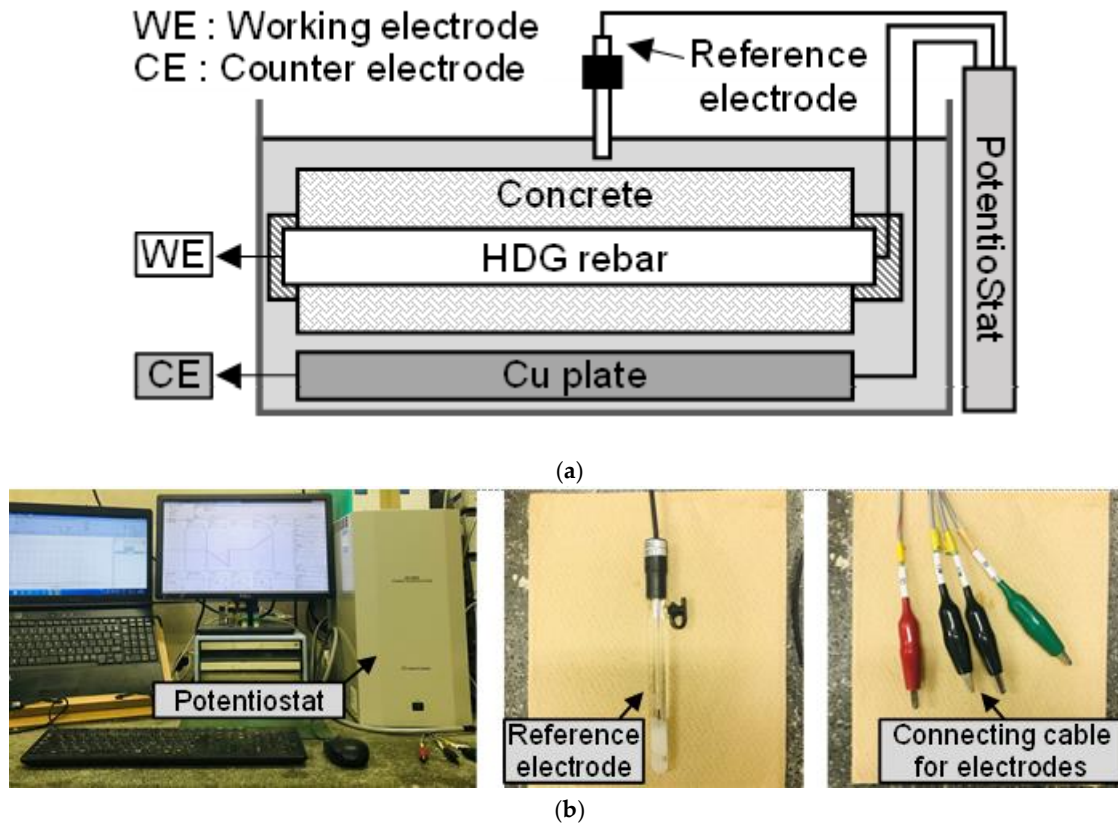


Figure 4. (a) Polarization test; (b) View of the polarization test outline and the main measurement devices.

Before polarization, the corrosion potential (hereafter, E_{corr}) was measured for 30 min. E_{corr} is defined as a potential, which is stable in its natural state. As a polarization condition, the scanning rate of the potential was 1 mV/s, the anodic polarization range was from E_{corr} to $E_{corr} + 250$ mV, and the cathodic polarization range was from E_{corr} to $E_{corr} - 250$ mV. The test was carried out in the order of anodic polarization → hold of polarization (300 seconds) → cathodic polarization. When the polarization was finished, a plot of the scanned potential (hereafter, E) and the measured current (hereafter, I) ($E - I$ plot) was drawn.

After the polarization, the electrochemical properties were evaluated based on the stern-geary equation [27], as shown in Equation (3). In calculating B , an $[E - \log I]$ plot was used to measure the anodic gradient (hereafter, β_a) and cathodic gradient (hereafter, β_c). β_a and β_c are located in the tafel region and generally appear as linear slopes. β_a was measured, where the potential is over +100 mV from E_{corr} . β_c was measured, where the potential is over -100 mV from E_{corr} . In calculating the polarization resistance (hereafter, R_p), it is expressed as an $\Delta E/\Delta I$ in $[E - I]$ plot. In this experiment, R_p was measured in a range from ($E_{corr} - 10$ mV) to ($E_{corr} + 10$ mV), which is known to show the linear slope [28–31].

$$i_{corr} = B \times R_p^{-1} = \{(\beta_a \times \beta_c) / 2.3 \times (\beta_a + \beta_c)\} \times R_p^{-1} \quad (3)$$

i_{corr} : Corrosion current density ($\mu\text{A}/\text{cm}^2$), B : Tafel constant (V), R_p : Polarization resistance ($\Omega \times \text{cm}^2$), β_a : Anodic gradient (V/decade), β_c : Cathodic gradient (V/decade).

2.4. Measurement of Remaining Coating Thickness

Figure 5 and Equation (4) indicate the process of measuring the remaining coating thickness. It compares the actual corrosion amount of zinc using DCA. Firstly, HDG rebar was taken out of the concrete. Secondly, referring to ISO 1460: 1992, weight measurements of HDG rebar, before (hereafter, W_1) and after (hereafter, W_2) the removal of the zinc coating, were conducted [32]. When measuring W_1 , the zinc product was removed using a metal brush. For the measurement of W_2 , a designated solution (more than 35 wt.% of HCl 500 mL + 500 mL of Distilled Water + 3.5 g of Hexamethylenetetramine ($\text{C}_6\text{H}_{12}\text{N}_4$)) was used to dissolve the full amount of zinc. After that, the surface of the substrate was dried, and W_2 was measured. Finally, the remained coating thickness (hereafter, $t_{remained}$) was calculated by Equation (4).

$$t_{remained} = \{(W_1 - W_2) / 7.2S\} \times 10^6 \quad (4)$$

$t_{remained}$: Remaining thickness of zinc coating (μm), W_1 : Weight of HDG rebar, before the removal of zinc coating (g), W_2 : Weight of HDG rebar, after the removal of zinc coating (g), 7.2: Density of zinc (g/cm^3), S : Surface area of HDG rebar (mm^2).

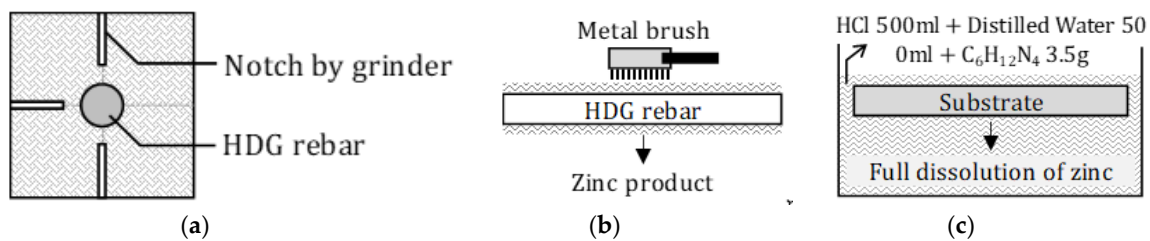


Figure 5. Specimen Treatment for Measuring the Remaining Coating Thickness. (a) Concrete cutting; (b) removing the zinc product and concrete on the surface (before measuring W_1); (c) removal of the remaining zinc coating on the substrate (before measuring W_2).

3. Results and Discussion

Table 4 indicates the electrochemical properties and corroded amount of all specimens, after the acceleration test. R_p was mainly discussed in relation to the evaluation of the corrosion behavior, and the estimated corrosion thickness (hereafter, $t_{corroded}$) was also calculated using Equation (4). When calculating $t_{corroded}$, the weight difference was $[W_0 - W_1]$. W_0 is the presumed weight of the uncorroded HDG rebar by its length ($= 1.56 \text{ g}/\text{mm}$). It was measured from 15 randomly chosen samples.

Table 4. Electrochemical properties and amount of corrosion of specimens, after the acceleration test.

No	Specimen	DCA ¹ (%)	E_{corr} ² (V)	R_p ³ ($K\Omega \times cm^2$)	i_{corr} ⁴ ($\mu A/cm^2$)	$t_{remained}$ ⁵ (μm)	$t_{corroded}$ ⁶ (μm)	Cracks on Concrete ⁷
1-1	W50-D160	25	-0.830	11.77	5.43	203.70	-54.29	
1-2		50	-0.963	13.50	4.74	188.37	-50.03	
1-3		75	-0.707	18.79	3.41	180.26	-36.09	
1-4		100	-0.590	27.53	2.32	159.11	-6.27	
2-1	W50-D80	25	-0.916	27.23	2.35	180.10	-40.33	Unfound
2-2		50	-0.810	41.88	1.53	178.12	-52.92	
2-3		75	-0.833	125.80	0.51	188.77	-55.62	
2-4		100	-0.957	77.29	0.83	154.84	-16.12	
3-1	W50-D20	25	-0.489	53.82	1.19	187.16	-48.30	
3-2		50	-0.397	69.47	0.92	170.08	-34.06	
3-3		75	-0.357	111.77	0.57	168.59	-31.86	
4-1	W83.5-D80	15	-0.882	19.63	2.87	123.60	23.31	Unfound
4-2		25	-0.931	23.26	2.42	111.43	37.40	
4-3		50	-0.644	56.81	0.99	89.95	70.05	Found
4-4		100	-0.549	69.13	0.81	97.63	79.07	Found
5-1	W83.5-D230-1	10	-0.463	10.20	5.52	Not measured		Unfound
5-2		25	-0.901	14.66	3.84	134.78	20.29	
5-3		50	-0.960	26.23	2.15	115.32	43.74	Found
5-4		75	-0.879	20.06	2.81	98.56	82.81	Found
5-5		100	-0.758	6.23	9.04	102.95	79.90	Found
6-1	W83.5-D230-2	20	-0.957	15.54	3.62	118.94	7.11	Unfound
6-2		50	-0.813	21.66	2.60	132.85	-0.73	
6-3		75	-0.884	158.00	0.36	101.00	52.44	Found

¹ Designed corrosion amount; ² Corrosion potential; ³ Polarization resistance; ⁴ Corrosion current density. In calculating i_{corr} , the average tafel constant (B) was used, which is 0.063 V on $w/c = 50\%$ specimens and 0.056 V on $w/c = 83.5\%$ specimens; ⁵ Remaining coating thickness ($= W_1 - W_2$); ⁶ Estimated corrosion thickness of zinc coating ($= W_0 - W_1$). (-) indicates the increase of thickness from the initial (uncorroded) state; ⁷ A crack, which appeared longitudinally with the rebar and broke the concrete surface.

3.1. Observation of Surface Changes of HDG Rebar

Figure 6 shows the surface of HDG rebar in $w/c = 50\%$ and 83.5% concrete, which corroded at 0.08 mA/cm^2 of applied current density. On each HDG rebar, the surface of both sides (top and bottom) were observed. Meanwhile, concerning other specimens that corroded at different applied current densities, the observation of the surface changes was similarly found to depend upon whether w/c is 50% or 83.5% .



DCA: 25% (26.32 mA × h/cm²)



DCA: 50% (52.63 mA × h/cm²)



DCA: 100% (105.26 mA × h/cm²)



(a)



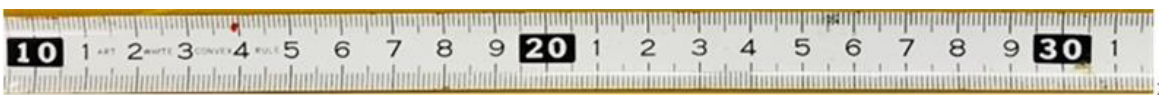
DCA: 25% (26.32 mA × h/cm²)



DCA: 50% (52.63 mA × h/cm²)



DCA: 100% (105.26 mA × h/cm²)



(b)

Figure 6. The surface of Hot-dip Galvanized (HDG) rebar, determined by an acceleration test at 0.08 mA/cm². (a) w/c = 50%; (b) w/c = 83.5%.

From the specimens of $w/c = 50\%$ concrete, the black-colored film was formed over the entire surface of rebar, which is presumed to be an oxide film. From the observation of the cross-section, the oxide film covered the zinc coating with, for example, a thin layer. This film appeared when DCA was 25%, which is the lowest total current amount. Additionally, it was maintained in a stable condition, until the DCA was 100%. While the (silver-colored) zinc coating partially remained when DCA was 25%, this coating was unseen after DCA was 50%. Meanwhile, zinc product was mainly formed on one side of the surface by covering the oxide film, and it increased with the total current amount. However, no corrosion of the substrate was found on all specimens in $w/c = 50\%$ concrete. While the total current amount was designed to corrode the entire thickness of the zinc coating at 100% of DCA, the zinc coating remained, and thus the sacrificial anodic reaction effectively functioned.

In the specimens of $w/c = 83.5\%$ concrete, the oxide film appeared as well. However, comparatively more zinc product was formed than in $w/c = 50\%$ and was found on both sides. After that, the substrate (red product) also corroded where the zinc product was formed. Meanwhile, concerning the apparent amount of zinc product, no remarkable difference was seen between DCA = 50% and 100%. This result indicated that, when zinc product generates more than the threshold amount on a particular area, the anti-corrosion effect of zinc no longer functions, and the steel substrate starts to corrode intensively. While there was a remaining zinc coating in another area, a noticeable formation of zinc product did not occur.

Concerning the corrosion product, it is known that the representative zinc product from HDG rebar is ZnO and $Zn(OH)_2$. They are loose and powdery minerals and appear as a white layer covering the surface [14,33–36]. Therefore, it was confirmed that the oxide film did not result from the reaction of zinc. Langill and Dugan [37] stated that an alloy content, such as silicon and phosphorus, is used to form a stable structure and sufficient thickness of zinc coating. In these alloy contents, silicon is a strong deoxidizing element and has a property of being combined with oxygen. Besides, in an investigation on Longbird bridge (Bermuda, 21-years-old) and Flatts bridge (Bermuda, 8-years-old), Stark et al. [9] reported that the surface of zinc coating turned black when the remaining zinc was 150 μm and 210 μm on each bridge, and both showed no corrosion of the substrate. While they were unable to determine which w/c was applied in those bridges, it is assumed that silicon in the zinc coating generated an anodic reaction to form the oxide film, irrespective of the w/c . For this reason, the corrosion of the zinc coating was delayed during the initial period of the acceleration test. Additionally, the zinc product of HDG rebar was found to be similar, when it was corroded by the acceleration test and in the actual corrosion environment.

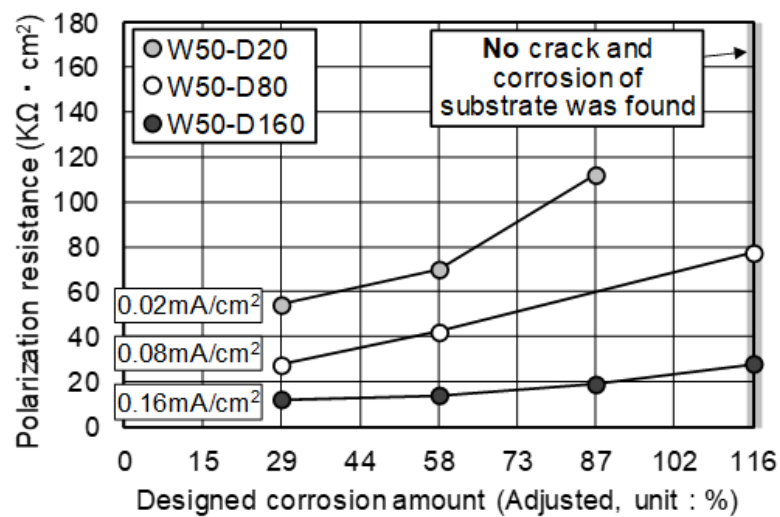
Concerning the corrosion behavior of HDG rebar by w/c , previous studies found that a high w/c accelerated the onset of the corrosion of HDG rebar [38–41]. Various w/c from 0.4 to 0.7 were investigated, and these studies aimed to evaluate either the corrosion current, weight loss or visual characteristics.

In the study by Clear et al. [38], slabs were cast with 0.4 and 0.5 w/c and immersed in a salt solution. As a result, the corrosion current in 0.5 w/c was 0.1 $\mu A/cm^2$, and it was nearly twice than in 0.4 w/c ($= 0.05 \mu A/m^2$). Additionally, Saiful Islam et al. [39] carried out an alternate wetting (using artificial seawater) and drying test with 0.4 and 0.48 w/c concrete cylinders, and the cover was 15, 25, and 40 mm. Specimens were exposed from 3 to 18 months. It was found that the weight loss of HDG rebar in 0.48 w/c was 0.12%, 0.095% and 0.032% at 15, 25, 40 mm covers. In 0.4 w/c , the weight loss was 0.11%, 0.08% and 0.038% with the same covers, which was a slightly reduced corrosion amount from 0.48 w/c . Meanwhile, Thangavel [40] investigated the corrosion resistance of HDG rebar (95 μm zinc thickness) with low-quality (0.68 w/c) and high-quality (0.5 w/c) concrete. Concrete that was chloride-contaminated and exposed by the full immersion of potable water and seawater was used for three years. The result found that 0.68 w/c concrete caused a rapid dissolution of zinc and the early corrosion of the substrate. Furthermore, Griffin [41] tested the concrete walls with 0.644 and 0.702 w/c , and the walls were approximately 1 m^2 , with a 25 mm cover. They were sprayed daily with seawater for 3 years. The result showed that, although 0.644 w/c inhibited the corrosion of HDG rebar, unlike 0.702 w/c , HDG rebar did not have a better anti-corrosion effect than non-galvanized rebar.

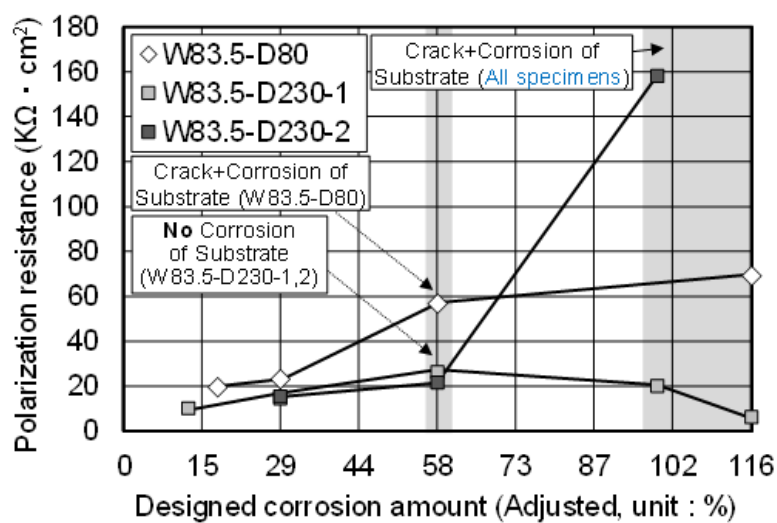
Therefore, based on previous studies and the result found in this experiment, it is expected that a high ratio of w/c concrete made HDG rebar corrode more quickly and terminated the anti-corrosion effect of the zinc coating. Additionally, it is expected that the corrosion behavior in w/c = 50% is closer to that of Longbird and Flatts bridges, which were referred to in this study. While there was a difference in the corroding extent, according to the w/c, the corrosion behavior of HDG rebar was similar and occurred in the following way: the initial dissolution of a certain amount of zinc → formation of the oxide film → increase of the zinc product to the entire surface → corrosion of the substrate.

3.2. Electrochemical Properties

Before discussing the experiment results, it was found that some data were scattered from the general tendency of the corrosion behavior. It is presumed that this result was due to the influence of some HDG rebar being damaged on its surface, while the fresh concrete was poured. For this reason, although specimens were prepared under the same condition, non-uniform corrosion was unexpectedly generated during the acceleration test. For this reason, Figures 7–9 presented the test results, showing a constant tendency.



(a)



(b)

Figure 7. (a) Behavior of R_p (w/c = 50% concrete); (b) Behavior of R_p (w/c = 83.5% concrete).

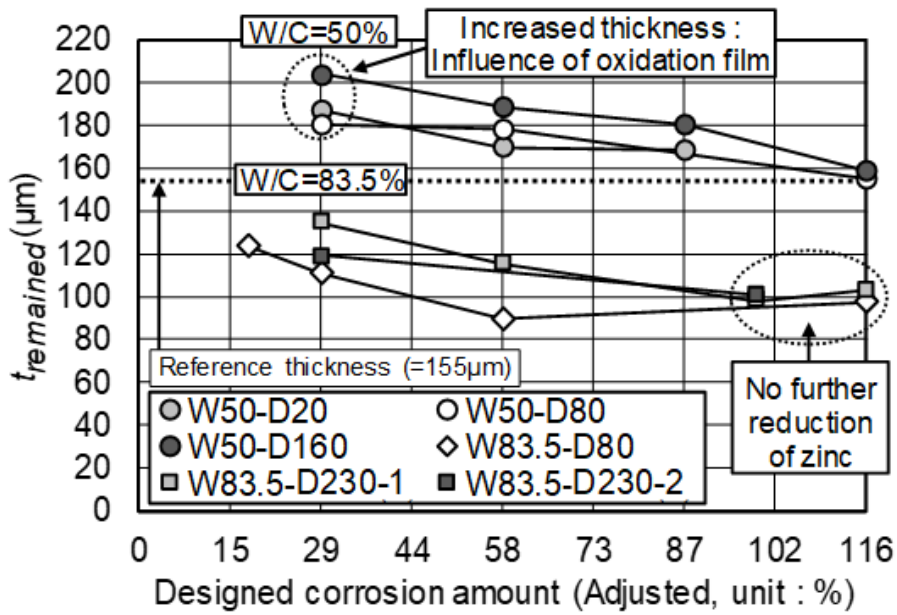
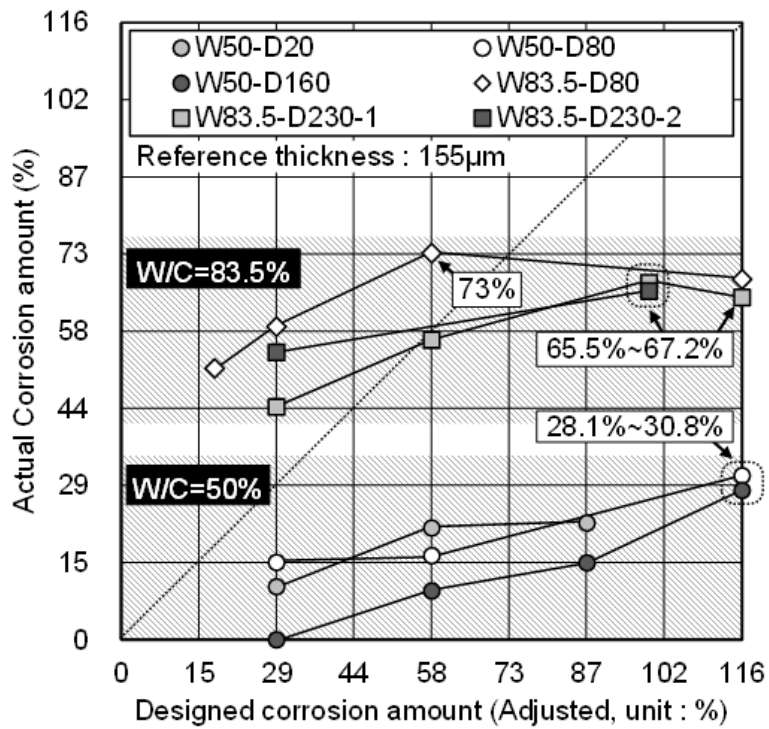
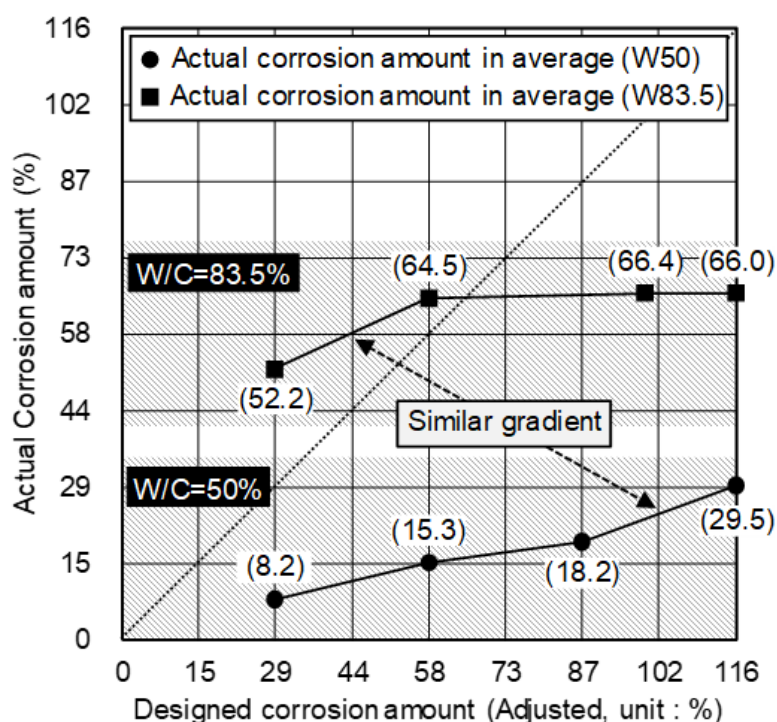


Figure 8. Remaining thickness of the zinc coating.



(a)

Figure 9. Cont.



(b)

Figure 9. Comparison of the actual and designed corrosion amounts. (a) Result for each specimen; (b) Average.

Figure 7 indicates the behavior of R_p in all specimens. Before discussing the corrosion behavior, the adjustment of DCA was considered because of the measurement difference in the reference thickness. It was 180 μm , when measured by the thickness meter. However, when the weight difference was measured using $[W_0 - W_2]$, it was calculated and found to be 155 μm by Equation (4). In this study, it was decided to adjust the reference thickness to 155 μm . This is the coating thickness, measured by the same method for evaluating the actual corrosion amount and DCA. Thus, if the reference thickness changed from 180 μm to 155 μm , DCA is increased to 1.16 times this value, because the total current amount was provided for corroding 180 μm of zinc. For example, 100% of DCA is adjusted to 116%. The adjusted DCA is presented in Figures 7–9.

In the specimens of $w/c = 50\%$ concrete, R_p gradually increased with the DCA. Besides, when the DCA is the same, R_p was higher when the HDG rebar was corroded in the lower applied current density. In the measurement of R_p , the detected current is the reaction of the surface of the metal. Thus, if a substance that shows less conductivity is formed on the surface, R_p tends to be increased. In Figure 6, the zinc product became denser, as the DCA was increased. When the DCA was the same, it was observed that the W50-D20 specimen showed comparatively more zinc product on the surface.

Yeomans [33] reported that the zinc corrosion products could migrate away from the rebar and into the adjacent concrete matrix, where they fill voids and microcracks. He also stated that zinc product causes very little physical disruption to the surrounding matrix, even though the active corrosion of the coating may be occurring. Additionally, Fratesi [42] suggested that the presence of these corrosion products and the filling of the pore space in the matrix may create a barrier in the matrix with reduced permeability. By referring to the previous studies, mentioned above, it is assumed that the zinc product mainly influenced the behavior of R_p in this experiment. The increasing amount of zinc product on the surface acted as a substance that resulted in a high R_p in the measurement result. Additionally, concerning the difference in the applied current density, the migration of zinc product affected its formation behavior. That is to say, the lower the applied current density, the more the zinc

product remained on the surface. Meanwhile, it was observed that ZnO, one of the zinc products, has no passivating properties [35,36]. However, whether the zinc product is ZnO or Zn(OH)₂ was not determined in this study. Instead, in order to confirm if the increasing R_p is related to the suppression of zinc corrosion, an evaluation of the actual corrosion amount was carried out.

In the specimens of $w/c = 83.5\%$ concrete, a gradual increase of R_p appeared, until DCA was 58%. Additionally, R_p was shown to be higher at a lower applied current density. This tendency was similar to the behavior in $w/c = 50\%$ concrete. However, after DCA = 58%, the specimens showed an unstable R_p . There was a decrease of R_p in the W83.5-D230-1 specimen or a sharp increase of R_p in the W83.5-D230-2 specimen, although these were identical samples. The W83.5-D80 specimen showed a decreased R_p slope.

In this stage, a longitudinal crack on the concrete surface was found, which broke the cross-section. This crack was due to the corrosion of the substrate and expansion of the rebar. It occurred mostly after DCA was 58%, and all of the specimens showed a crack at 99% DCA. Therefore, it is assumed that the anti-corrosion effect of HDG rebar due to zinc coating was terminated at 58%–99% DCA. Additionally, while the increasing R_p shows a gradual slope, the sacrificial anodic reaction of zinc is expected to be functioning effectively.

3.3. t_{remained} on HDG Rebar

Figure 8 indicates the t_{remained} of all specimens, after the acceleration test. Meanwhile, in measuring t_{remained} , W_1 included the oxide film due to its adhesiveness. After the removal of the zinc product, it was uneasy to remove the oxide film using a metal brush. For this reason, t_{remained} included the thickness of the oxide film as well. In this graph, the thickness of the non-corroded zinc coating was presented as the reference (= 155 μm).

From the specimens of $w/c = 50\%$ concrete, t_{remained} was found to be higher than the reference thickness, but it decreased with the DCA. Besides, when DCA reached 116%, the t_{remained} of all specimens were almost similar, regardless of the applied current density. On the other hand, in $w/c = 83.5\%$ concrete, t_{remained} was lower than the reference thickness, although it included the oxide film. Additionally, when the decrease of t_{remained} reached 100 μm at DCA = 99%, despite the increase of DCA, there were no more noticeable thickness reductions.

The result of t_{corroded} was considered to indicate the behavior of t_{remained} . The value of t_{corroded} indicates that (+) is a decrease and (–) is an increase of the thickness, in relation to the initial thickness. From the result of $w/c = 50\%$ concrete, the increase of thickness at DCA = 29% was $-40.33\sim-54.29\ \mu\text{m}$ for each specimen. This increase was due to the oxide film, and it was mostly the maximum. Therefore, it is assumed that the oxide film was fully formed, before the active corrosion of zinc, as a delaying effect in the initial stage, and it is maintained at a constant thickness. In $w/c = 50\%$ concrete, the influence of the oxide film appeared when DCA = 29%. In $w/c = 83.5\%$ concrete, the delaying effect was assumed to exist when DCA was less than 29%. Therefore, referring to t_{corroded} , which appeared in $w/c = 50\%$ concrete at DCA = 29%, it is predicted that the thickness of the oxide film is 47.64 μm , regardless of the w/c .

Meanwhile, in the scope of this study, the difference in the applied current density barely showed the influence on t_{remained} . It was mainly affected by the total current amount. Thus, if HDG rebar was embedded in the same w/c concrete and had a certain amount of the total amount of corrosion, the actual corrosion amount was expected to be similar. Moreover, from the result of $w/c = 83.5\%$ concrete, even though t_{remained} did not reach 0 μm , the early end of the anti-corrosion effect was confirmed. This result corresponded well with the surface change of HDG rebar, which was discussed in Figure 6. Additionally, it was clarified that the increase of R_p , which showed a gradual slope in Figure 7, did not suppress the corrosion of zinc. The behavior of R_p was only relevant to the property of the zinc product.

3.4. Comparison of the Actual Corrosion Amount and the DCA of Zinc

Figure 9 shows a comparison of the actual corrosion amount and the DCA of all specimens. The actual corrosion amount was calculated by Equation (5), which considered the predicted thickness of the oxide film and the reference thickness. [$t_{\text{remained}} - 47.64 \mu\text{m}$] was chosen as a remained coating thickness of zinc, and 155 is the reference thickness (μm) of HDG rebar, which is not a corroded condition. In order to avoid a confusion of expression related to the corrosion amount, the (actual corrosion amount) is hereafter referred to as “ACA”.

$$\text{Actual corrosion amount (\%)} = \{1 - (t_{\text{remained}} - 47.64)/155\} \times 100 \quad (5)$$

In $w/c = 50\%$ concrete, the maximum actual corrosion amount (ACA) was about 29.5% against 116% of DCA. The ACA of zinc was lower than DCA over the entire period of the acceleration test. Besides, the average of all specimens at each DCA mostly showed an ACA that was about 1/4 times lower. Therefore, in the scope of this study, the HDG rebar in $w/c = 50\%$ concrete effectively protected the corrosion of the substrate and showed a constant anti-corrosion effect.

In $w/c = 83.5\%$ concrete, the ACA of zinc was higher than the DCA during 0%~58%. The reason was that the corrosion reaction quickly proceeded during 0%~29%. After 58% of DCA, the corrosion of zinc did not proceed noticeably and showed the end of the anti-corrosion effect. While there was a reduction of ACA on W83.5-D80 (DCA = 58% \rightarrow 116%) and W83.5-D230-1 (DCA = 99% \rightarrow 116%) specimens, it was regarded as an error due to the condition, which tested only a single specimen. Therefore, it is expected that the HDG rebar in $w/c = 83.5\%$ concrete reached the threshold amount of zinc corrosion, and it was about 66%.

Meanwhile, in $w/c = 50\%$ concrete, ACA did not reach the end of the anti-corrosion effect in this study. However, during 29%–58% of DCA in $w/c = 83.5\%$ concrete, the gradient of the average ACA appeared to be similar to that in $w/c = 50\%$ concrete, when DCA = 87%–116%. This result indicates that the corrosion rate becomes constant at least after about 50% of ACA, even though w/c is different. From this result, unless the HDG rebar in $w/c = 50\%$ concrete shows a rapid increase of ACA, it is assumed that the anti-corrosion effect of zinc will continue until about 66% of ACA. By referring to the experiment result in this study, a future study is required to impress more of the current amount, until the corrosion of the substrate appears, in order to clarify the threshold amount of zinc corrosion.

3.5. Correspondence between the Field Performance and the Experimental Result of the Acceleration Test

In the experimental result of this study, specimens of $w/c = 83.5\%$ concrete reached the end of the anti-corrosion effect. The W83.5-D80 specimen showed 73% of ACA, and W83.5-D230 specimens showed 66% of ACA, when it was at the maximum. Meanwhile, in the study of Niwa et al. [6], ACA was 43% when corrosion of the substrate occurred. This result was tested using the acceleration test. Additionally, from the field performance of HDG rebar in Tioga bridge, the remaining zinc thickness was 38 μm when the substrate was corroded [12]. In order for the acceleration test to be useful in the evaluation of HDG rebar, it is necessary to confirm that the experiment results correspond with the result in the actual corrosion environment. Accordingly, the remaining zinc thickness at the stage when HDG rebar showed corrosion of the substrate was evaluated at each current density of the acceleration test. This is because the initial zinc thickness can differ, according to the type of HDG rebar. For this reason, how to predict the anti-corrosion performance by ACA is unclear.

Figure 10 indicates the correlation between the applied current density and the remaining zinc thickness. In this graph, the result for the field performance was regarded as not being corroded by the impression of the applied current density ($=0 \text{ mA/cm}^2$). Concerning the results achieved in this study, 73% of ACA at 0.08 mA/cm^2 was converted to 42 μm of the remaining zinc thickness ($= 155 \mu\text{m} \times 0.23$). In the same way, 66% of ACA at 0.23 mA/cm^2 was converted to 53 μm ($= 155 \mu\text{m} \times 0.34$). Concerning the result of Niwa et al., 43% of ACA at 0.625 mA/cm^2 was converted to 87 μm ($= 153 \mu\text{m} \times 0.57$).

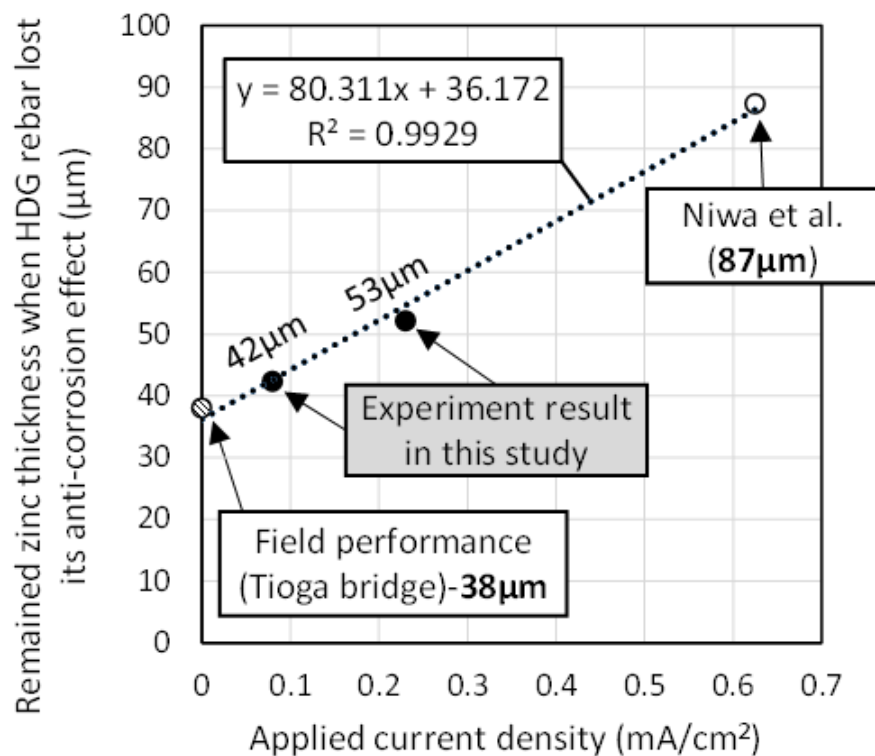


Figure 10. Correlation between the applied current density and the remaining zinc thickness in each corrosion environment (the acceleration test and the field performance).

As a result, the regression equation showed a well-fitted correspondence between the acceleration test and the actual corrosion environment in terms of the remaining zinc thickness, which was a linear relationship. Moreover, the extent of the applied current density was influential in causing the early end of the anti-corrosion effect. It is expected that lowering the applied current density will result in a more suitable test condition. In this graph, it is recommended that the acceleration test needs to be carried out below 0.1 mA/cm^2 . From this result, the acceleration test was found to be useful.

Meanwhile, concerning the data referred to in this study, it was not widely investigated whether this linear relationship is expected to appear in the range of 0.23 mA/cm^2 – 0.625 mA/cm^2 . Therefore, in order to clarify a more suitable range for the acceleration test condition, further experimental validation at various applied current densities is necessary.

4. Conclusions

In this study, the usability of the acceleration test was investigated, considering if it is a suitable method for evaluating the anti-corrosion behavior of HDG rebar in concrete. By referring to the field performance of HDG rebar, which showed the corrosion of the substrate, and the previous study, which impressed the high rate of the acceleration condition, a comparatively low rate of the applied current density was used as a variable for experimentation. HDG rebar was embedded in $w/c = 50\%$ and 83.5% concrete, and the total current amount was impressed to corrode the full amount of zinc coating.

- Concerning the observation of the surface change, a high ratio of w/c concrete made HDG rebar more easily corroded. Additionally, the further generation of zinc product did not proceed, after the corrosion of the substrate. The oxide film formed on HDG rebar showed a delaying effect of zinc corrosion in the initial stage, and it maintained a constant thickness, once it was fully formed.

2. As long as there was no corrosion of the substrate, HDG rebar showed a gradual increase of R_p , as corrosion proceeded. Additionally, when the total current amount was the same, R_p was relatively high in the lower applied current density. This behavior was mainly influenced by the apparent amount of zinc product, formed on the surface.
3. While the applied current density was different, if the w/c was the same, the actual corrosion amount was expected to be similar in this study. Additionally, even though there was some remaining zinc coating, once the corrosion of the substrate proceeded, HDG rebar stopped functioning the sacrificial anodic reaction of zinc.
4. The corrosion behavior of HDG rebar, which appeared in the acceleration test, was found to be similar to that in the actual corrosion environment. While the remaining zinc thickness at the time that the corrosion of the substrate started was thicker than the result of the field performance, a linear relationship was confirmed between the applied current density and the remaining zinc thickness. The higher the applied current density, the earlier the termination of the anti-corrosion effect, which caused a higher remaining zinc thickness. Therefore, in this study, it is recommended that the acceleration test be carried out below 0.1 mA/cm².
5. In conclusion, while further experimental validation at various applied current densities is necessary, the acceleration test using impressed anodic current is expected to be appropriate for evaluating the durability of corroded HDG rebar, while the zinc coating is causing an anti-corrosion effect.

Author Contributions: Conceptualization, H.-b.C.; methodology, H.-b.C.; writing—original draft preparation, H.-b.C.; writing—review and editing, Y.N.; supervision, M.K.; project administration, M.K.

Funding: This research received no external funding.

Conflicts of Interest: The authors declare no conflict of interest. The funders had no role in the design of the study; in the collection, analyses, or interpretation of data; in the writing of the manuscript, or in the decision to publish the results.

References

1. Yeomans, R.S. Galvanized Steel in Concrete: An Overview. In *Galvanized Steel Reinforcement in Concrete*, 1st ed.; Yeomans, R.S., Ed.; Elsevier: Oxford, UK, 2004; Chapter 1; pp. 1–30.
2. Andrade, C.; Alonso, C. Electrochemical Aspects of Galvanized Reinforcement Corrosion. In *Galvanized Steel Reinforcement in Concrete*, 1st ed.; Yeomans, R.S., Ed.; Elsevier: Oxford, UK, 2004; Chapter 5; pp. 111–144.
3. Sistonen, E. Service Life of Hot-dip Galvanized Reinforcement Bars in Carbonated and Chloride-contaminated Concrete. Ph.D. Thesis, Helsinki University of Technology, Espoo, Finland, 2009.
4. Figueira, R.B.; Silva, C.J.R.; Pereira, E.V.; Salta, M.M. Corrosion of Hot-dip Galvanized Steel Reinforcement. *Corros. Prot. Mater.* **2014**, *33*, 44–54.
5. Choe, H.B.; Nishio, Y.; Kanematsu, M. Evaluation of Galvanic Corrosion between Hot-dip Galvanized Steel and Ordinary Steel Rebar in Concrete Environment. In Proceedings of the 8th International Conference of Asian Concrete Federation, Fuzhou, China, 4–7 November 2018.
6. Niwa, A.; Choe, H.B.; Kanematsu, M. The Bonding Performance of Hot-dip Galvanized Steel in the Concrete with regard to Its Corrosion Behavior. In Proceedings of the Japan Concrete Institute, Kobe, Japan, 4–6 July 2018. (In Japanese).
7. Kouril, M.; Pokorný, P.; Stouřil, J. Corrosion Mechanism and Bond-strength Study on Galvanized Steel in Concrete Environment. *Corros. Sci. Technol.* **2017**, *16*, 69–75.
8. Farina, S.B.; Duffo, G.S. Corrosion of Zinc in Simulated Carbonated Concrete Pore Solutions. *Electrochim. Acta* **2007**, *52*, 5131–5139. [[CrossRef](#)]
9. Stark, D.; Perenchio, W.F. *The Performance of Galvanized Reinforcement in Concrete Bridge Decks*. ILZRO Project ZE-206; International Lead Zinc Research Organization: Durham, NC, USA, 1975.
10. Stark, D. *Galvanized Reinforcement in Concrete Containing Chlorides*. ILZRO Project ZE-247; International Lead Zinc Research Organization: Durham, NC, USA, 1978.

11. Stark, D. *Evaluation of the Performance of Galvanized Reinforcement in Concrete Bridge Decks*. ILZRO Project ZE-320; International Lead Zinc Research Organization: Durham, NC, USA, 1982.
12. Stejskal, B.G. *Evaluation of the Performance of Galvanized Steel Reinforcement in Concrete Bridge Decks*. CTL Project 050324; Construction Technology Laboratories Inc.: Skokie, IL, USA, 1992.
13. Olson, C.A.; Nagi, M.A. *Evaluation of the Performance of Galvanized Steel in Concrete Bridge Decks*. ILZRO PROJECT ZC-10; Construction Technology Laboratories, Inc.: Skoki, IL, USA, 2002.
14. Belaid, F.; Arligue, G.; Francois, R. Corrosion products of galvanized rebars embedded in chloride containing concrete. *Corrosion* **2000**, *56*, 960–965. [[CrossRef](#)]
15. Care, S.; Nguyen, T.Q.; L'Hostis, V.; Berthaud, Y. Mechanical Properties of the Rust Layer Induced by Impressed Current Method in Reinforced Mortar. *Cem. Concr. Res.* **2008**, *38*, 1079–1091. [[CrossRef](#)]
16. Yuan, Y.; Ji, Y.; Shah, S.P. Comparison of Two Accelerated Corrosion Techniques for Concrete Structures. *ACI Struct. J.* **2007**, *104*, 344–347.
17. Vu, K.; Stewart, M.G.; Mullar, J. Corrosion-Induced Cracking: Experimental Data and Predictive Models. *ACI Struct. J.* **2005**, *102*, 719–726.
18. Congqi, F.; Karin, L.; Liuguo, C.; Chaoying, Z. Corrosion Influence on Bond in Reinforced Concrete. *Cem. Concr. Res.* **2004**, *34*, 2159–2167.
19. El Maaddawy, T.A.; Soudki, K.A. Effectiveness of Impressed Current Technique to Simulate Corrosion of Steel Reinforcement in Concrete. *J. Mater. Civ. Eng.* **2003**, *15*, 41–47. [[CrossRef](#)]
20. Abdullah, A.A.; Ahmad, S.A.; Abdur, R.A.; Fahd, H.D.; Rasheeduzzafar. Effect of Reinforcement Corrosion on Flexural Behavior of Concrete Slabs. *J. Mater. Civ. Eng.* **1996**, *8*, 123–127.
21. ILZRO. *Galvanized Reinforcement for Concrete*; International Lead Zinc Research Organization: Durham, NC, USA, 1981.
22. Cornet, I.; Bresler, B. Critique of testing procedures related to measuring the performance of galvanized steel reinforcement in concrete. In *Corrosion of Reinforcing Steel in Concrete (ASTM STP 713)*; Tonini, D.E., Gaidis, J.M., Eds.; American Society for Testing and Materials: Philadelphia, PA, USA, 1980; pp. 160–195.
23. Bresler, B.; Cornet, I. Galvanized steel reinforcement in concrete. In Proceedings of the 7th Congress, International Association of Bridge and Structural Engineers, Rio de Janeiro, Brazil, 10–16 August 1964.
24. Bresler, B.; Cornet, I. *Corrosion Protection of Steel in Concrete and Tentative Recommendations for Use of Galvanized Steel Reinforcement in Concrete*; ILZRO Report TS-69-06; International Lead Zinc Research Organization: Durham, NC, USA, 1969.
25. Cornet, I.; Bresler, B. Corrosion of steel and galvanized steel in concrete. *Mater. Prot.* **1966**, *5*, 69–72.
26. Cornet, I.; Bresler, B.; Ishikawa, T. Mechanism of steel corrosion in concrete structures. *Mater. Prot.* **1968**, *7*, 44–46.
27. ASTM G102-89 (2015) e1. *Standard Practice for Calculation of Corrosion Rates and Related Information from Electrochemical Measurements*; ASTM International: West Conshohocken, PA, USA, 2015.
28. Poursaee, A. Potentiostatic Transient Technique, A Simple Approach to Estimate the Corrosion Current Density and Stern-gearly Constant of Reinforcing Steel in Concrete. *Cem. Concr. Res.* **2010**, *40*, 1451–1458. [[CrossRef](#)]
29. Badea, G.E.; Caraban, A.; Sebesan, M.; Dzitac, S.; Cret, P.; Setel, A. Polarization Measurements used for Corrosion Rates Determination. *J. Sustain. Energy* **2010**, *1*, 2067–5538.
30. Kelly, G.R. Electrochemical thermodynamics and kinetics of relevance to corrosion. In *Electrochemical Techniques in Corrosion Science and Engineering*, 1st ed.; Kelly, G.R., Scully, R.J., Shoesmith, W.D., Buchheit, G.R., Eds.; Marcel Dekker: New York, NY, USA, 2003; Chapter 2; pp. 9–54.
31. Andrade, C.; Alonso, C.; Gulikers, J.; Polder, R.C.; Vennesland, O.; Salta, M.; Raharinaivo, A.; Elsener, B. Test Methods for On-site Corrosion Rate Measurement of Steel Reinforcement in Concrete by Means of the Polarization Resistance Method. *Mater. Struct.* **2004**, *37*, 623–643. [[CrossRef](#)]
32. ISO. 1460: 1992. *Metallic Coatings—Hot Dip Galvanized Coatings on Ferrous Materials—Gravimetric Determination of the Mass per Unit Area*; ISO: Geneva, Switzerland, 1992.
33. Yeomans, S.R. *Corrosion of the Zinc Alloy Coating in Galvanized Reinforced Concrete*; NACE Corrosion: Houston, TX, USA, 1998.
34. Hoke, J.H.; Pickering, H.W.; Rosengarthm, K. *Cracking of Reinforced Concrete*. ILZRO Project ZE-271; International Lead Zinc Research Organization: Durham, NC, USA, 1981.

35. Blanco, M.T.; Andrade, C.; Macias, A. SEM study of the corrosion products of galvanized reinforcements immersed in solutions on the pH range 12.6 to 13.6. *Br. Corros. J.* **1984**, *19*, 41–48. [[CrossRef](#)]
36. Macias, A.; Andrade, C. Stability of the calcium hydroxizincate protective layer developed on galvanized reinforcements after a further increase of the pH value. *Mater. Constr.* **1986**, *36*, 19–27.
37. Langill, T.J.; Dugan, B. Zinc Materials for Use in Concrete. In *Galvanized Steel Reinforcement in Concrete*, 1st ed.; Yeomans, S.R., Ed.; Elsevier: Oxford, UK, 2004; Chapter 4; pp. 87–109.
38. Clear, K.C.; Virmani, Y.P.; Jones, W.; Jones, D. *Time-To-Corrosion of Reinforcing Steel in Concrete: Vol.4. Galvanizing Reinforcing Steel*; FHWA Report No. FHWA/RD-82/028; Federal Highway Administration: Washington, DC, USA, 1981.
39. Saiful Islam, M.D.; Kaushik, S.K. A study of corrosion of reinforced concrete in a simulated tropical marine environment. In *Corrosion and Corrosion Protection of steel in Concrete*; Swamy, N.R., Ed.; Sheffield Academic Press: Sheffield, UK, 1994; Volume 2, pp. 1267–1276.
40. Griffin, D.F. *Effectiveness of Zinc Coating on Reinforcing Steel in Concrete Exposed to a Marine Environment*; Technical Note N-1032; Naval Civil Engineering Laboratory: Port Hueneme, CA, USA, 1969.
41. Thangavel, K.; Rengaswamy, N.S.; Balakrishnan, K. Corrosion resistance of galvanized steel in concrete. *Mater. Perform.* **1995**, *34*, 59–63.
42. Fratesi, R.; Moriconi, G.; Coppola, L. The influence of steel galvanization on rebar behavior in concrete. In *Corrosion of Reinforcement in Concrete Construction*; Page, C.L., Bamforth, P.B., Figg, J.W., Eds.; Royal Society of Chemistry, Special Publication No 183, Royal Society of Chemistry: London, UK, 1996.



© 2019 by the authors. Licensee MDPI, Basel, Switzerland. This article is an open access article distributed under the terms and conditions of the Creative Commons Attribution (CC BY) license (<http://creativecommons.org/licenses/by/4.0/>).